



D2.1 Data from Laboratory Experiments

Grant Agreement number	675675
Project Acronym	COMPLETE
Project Title	Cloud-MicroPhysics-Turbulence-Telemetry
Funding Scheme	Marie Skłodowska Curie Actions – ITN - ETN
Version date of the Annex I against which the assessment will be made	29/05/2017
Start date of the project	01/06/2016
Due date of the deliverable	September 2020
Actual date of delivery	June 2020
Lead beneficiary	ICL
Dissemination level of the deliverable	Public

Coordinator and main scientific representative of the project

Prof. Daniela Tordella
Politecnico di Torino
DISAT, Department of Applied Science and Technology
Phone: 0039 011 090 6812
E-mail: daniela.tordella@polito.it, complete-network@polito.it

Project website: <https://www.complete-h2020network.eu/>

D2.1 Data from Laboratory Experiments

A planar jet flow is generated using a centrifugal blower which collects air from the environment and then forces it into a plenum chamber. In order to reduce the inflow turbulence intensity level and remove any bias due to the feeding circuit, the air passes through two sets of flow straighteners before entering a convergent duct (having area ratio equal to about 8). At the end of the duct there is a letterbox slit with aspect ratio $s/h = 31$ and $h = 15\text{mm}$ (see Figure 1). Figure 1 includes a schematic of the contoured inlet: in order to produce a top hat velocity profile at the jet exit ($x = 0$), the two longest sides of the slit are filleted with a radius $r = 2h$. The jet exhausts into ambient air and is confined in the spanwise direction by two perspex walls of size $100h \times 100h$ placed in $x - y$ planes. The aspect ratio $s/h = 31$ is sufficiently large to ensure that the flow can be considered planar as documented in the published literature. Furthermore, the effect of the boundary layer which develops on the bounding perspex walls is estimated to affect less than 3% of the overall spanwise extent at $100h$ from the jet exit section. The jet rig was located in a room much larger in all directions than the jet width δ at $x = 100h$, so that the effects of the ceiling, floor and room walls on the entrainment and development of the jet flow are reduced to a minimum. The inlet velocity was set at 20m/s and was stabilized using a PID feedback controller which takes as input the thermo-fluid-dynamic conditions of the flow measured by a thermocouple and a Pitot tube. The thermocouple measures the temperature of the working fluid about 5 cm upstream of the letterbox slit in the convergent part of the nozzle, whilst the Pitot tube is located such that the pressure measurements are carried out within the potential core of the jet flow. These data are acquired using a Furness Control micromanometer FCO510, then manipulated by the in house PID controller which outputs the voltage to be supplied to the blower's driver in order to achieve the desired flow speed.

We performed stereoscopic PIV (stereo-PIV) at four different streamwise locations to determine the kinematic and dynamic properties of the TNTI.

A dual cavity/double pulsed Nd:YAG laser (200mJ/pulse , 15Hz frequency, time separation between two pulses set to $90\ \mu\text{s}$) was used to produce a laser sheet that illuminates cross sections of the planar jet flow in the $y-z$ plane at four different streamwise locations, namely $x/h = 20, 30, 40, 50$. The two cameras (equipped with 100mm Macro lenses and Scheimpflug mounts) were located on either sides of the laser, imaging an area extending for $8h \times 6h$ in the $y-z$ plane, starting from $y = 0$ (see figure 1).

We perform streamwise derivatives of average quantities by also acquiring stereo-PIV images at two $y-z$ planes displaced by $\pm 0.3h$ in the x direction from each measurement plane. This results in 4500 images for each of the four measurement planes, which ensures convergence of the relevant statistics. The cross-correlation is operated using an iterative procedure with a final interrogation window size of 32×32 pixels with 75% overlap. Both raw images and velocity fields are interpolated using spline functions. A Blackman filtering is applied to tune the spatial resolution. The resulting vector pitch is 5η at $x/h = 20$ and reduces to 2.5η at $x/h = 50$.

The data are stored as raw images and as velocity fields and can be made available upon request.

A sample of the data obtained can be seen in figure 2.

Reference: Cafiero, G & Vassilicos, J.C. 2020 Non-equilibrium scalings of the turbulent/non turbulent interface speed. Preprint submitted for publication.

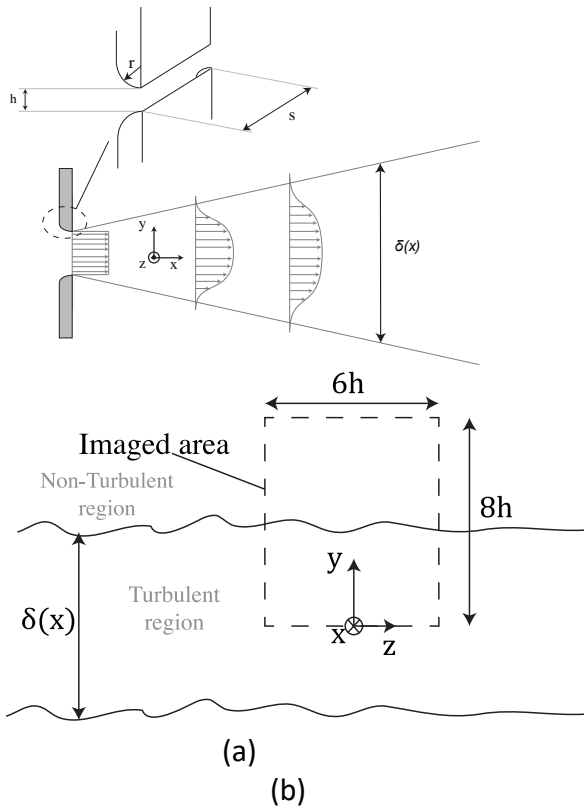
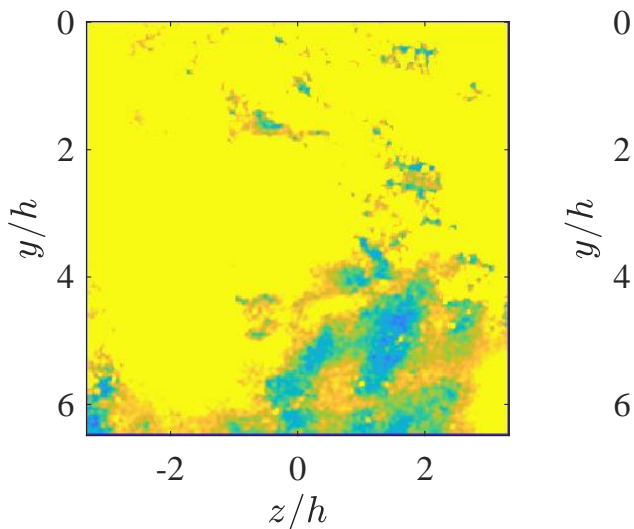


Figure 1: a) Schematic representation of the jet flow, with indication of the reference frame; b) cross section of the jet flow at a generic streamwise distance x , with indication of the imaged area $0 \leq y \leq 8h$, $-3h \leq z \leq 3h$. The two wiggly lines at the top and bottom represent the intersection of the Turbulent/Non-Turbulent Interface with the y - z plane at position x .



(a)
(b)
Figure 2: a) Contour representation of an instantaneous realization of the flow color coded according to turbulent kinetic energy values (from 0 in blue to 0.045 in yellow). b) Edge detection using a 0.04 value. Data are measured at $x/h=50$.